# HIGH HARMONICS FROM GAS, A SUITABLE SOURCE FOR SEEDING FEL FROM THE VACUUM-ULTRAVIOLET TO SOFT X-RAY REGION

G. Lambert, B. Vodungbo, J. Gautier, A. Sardinha, F. Tissandier, Ph. Zeitoun, S. Sebban, V. Malka,
LOA ENSTA-Paristech Palaiseau, France
M.E. Couprie, M. Labat, O. Chubar, Synchrotron Soleil, Gif-sur-Yvette, France
T. Hara, H. Kitamura, T. Shintake, Y. Tanaka, T. Tanikawa, SPring-8/RIKEN Harima Institute, Hyogo, Japan
D. Garzella, B. Carré CEA, DSM/SPAM, Gif-sur-Yvette, France
J. Luning, LCPMR, Paris
C.P. Hauri, Paul Scherrer Institute, Villigen, Switzerland
M. Fajardo, Centro de Física dos Plasmas / Instituto Superior Técnico, Lisboa, Portugal

*Abstract*

FEL have been recently evolving very fast from vacuum-ultraviolet to soft X-ray region. Once seeded with high harmonics generated in gas, these light sources deliver amplified emissions with properties which are, for most of them, directly linked to the injected harmonic beam, e.g. the ultrashort pulse duration for FEL and the high temporal and spatial degree of coherence. Since the last two years the developments of techniques for improving the harmonic properties for seeding FEL lead to major results on tunability, intensity, repetition rate and polarization. Actually harmonics are nowadays used for numbers of applications, before limited to FEL facility. Also, FEL based on harmonic seeding can benefit from the natural synchronization between the FEL, the harmonic and the laser used for generation, which makes it a perfect candidate for pump-probe experiment with fs resolution.

## INTRODUCTION

Seeding Free-Electron Lasers (FEL) with High order Harmonics (HH) generated in gas from the VUV (Vacuum Ultra Violet, 80-160 nm) to the soft X-ray (10-40 nm) region (also called here XUV for simplicity) is a quite recent but emerging topic. Indeed, it has already opened significant perspectives for developing the future ultimate relatively compact intense fully coherent jitter-free and aberration-free source in order to observe the ultrafast dynamics of matter at nanometre scale. Seeding relies on benefits from the high-quality properties of the HH source, particularly the ultrashort pulse duration or the high degree of spatial and temporal coherence.

Essentially, the seeding configuration in FEL is a direct evolution of the classical Self Amplified Spontaneous Emission (SASE) [1], which provides a very high brightness emission ($10^{12}$ photons per pulses of less than 100 fs duration, i.e. multi GW peak power) at rather high repetition rate and at short wavelengths (with important spectral tuning) with variable polarization, good wavefront properties [2] and spatial coherence [3] but with a limited temporal coherence [4]. The spectral and temporal profiles are typically composed of a series of randomly distributed spikes, reflecting the stochastic nature of the SASE generation process that is amplification of noise. In seeding arrangements, the amplification is triggered by the harmonic seed rather than the noise floor leading to strong and coherent amplified FEL radiation. The basic of the principle has been demonstrated some years ago [5] in IR, with $CO_2$ and Ti: Sa lasers, then in UV using crystals for frequency multiplication. Yet, since the beginning of this century, novel linear accelerator-based single-pass FEL sources in the VUV to soft-X ray have been emerged around the world (Flash [6] at 4.1 nm, SCSS Test Accelerator [7] at 49 nm, and SPARC [8] at 133 nm), it was needed to use new efficient fully coherent femtosecond laser sources in this spectral range for seeding FEL. High harmonics generated from gas have been then proposed.

## HIGH HARMONIC GENERATION

The harmonic generation in gas results from the strong non linear polarisation induced on the rare gases atoms, such as Ar, Xe, Ne and He, by the focused intense electromagnetic field $E_{Laser}$ of a "pump" laser at peak power about $10^{14}$ $W.cm^{-2}$. The most important characteristics of the process are given by the three-step semi-classical model illustrated in figure 1.

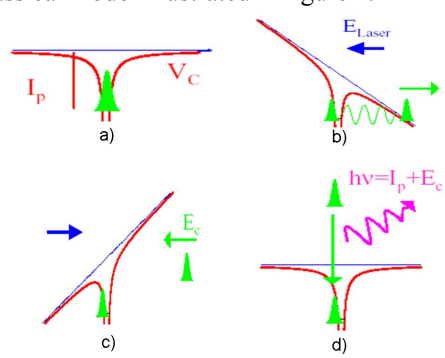


Figure 1: Three-step semi-classical model a) initial state of the gas atom b) electron tunnelling c) gain of kinetic energy $E_C$ d) electron absorption and photon emission. $I_P$ is the ionization potential of the gas.

ISBN 978-3-95450-117-5

As the external electromagnetic field strength is comparable to the internal static field $V_c$ of the atom in the interaction region close to laser focus, atoms ionize by tunnelling of the electrons. The ejected free electrons, far from the core, are then accelerated in the external laser field and gain in kinetic energy $E_C$. Those which are driven back close to the core can either be scattered or recombine to the ground state emitting a burst of XUV photons every half-optical cycle. This gives in the spectral domain a superposition of high order odd harmonics, separated by twice the fundamental energy (figure 2).

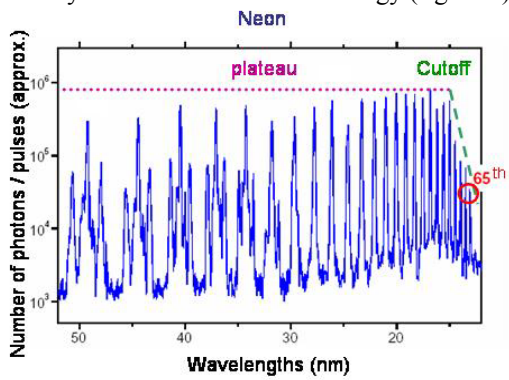


Figure 2: Typical high harmonics spectrum in Ne.

Even if the conversion rate of this technique is relatively weak ($10^{-4}$-$10^{-7}$), the characteristic distribution of intensities is almost constant with harmonic order into the "plateau" region. For higher orders, the conversion rate and consequently the intensities decrease rapidly in a zone called "cut-off" region. Its upper spectral limit is given by $E_{cutoff} = I_P + 3.2\ U_P$. $E_{cutoff}$ is the "cut-off" photon energy, $U_P$ is the ponderomotive potential and $U_P\ \alpha\ I_{pump}\ \lambda^2_{pump}$, with $I_{pump}$ the focused intensity, $\lambda_{pump}$ the wavelength of the pump and finally 3.2 corresponds to the maximum of kinetic energy which can be reached by the electron. In the regime, where atoms are not ionized, the lighter the gas, the higher the ionization potential and the laser intensity, and consequently the higher the cut-off energy. The maximum number $N_{max}$ of orders can be deduced by: $N_{max} \approx E_{cutoff}/h\upsilon_{pump}$, where $\upsilon_{pump}$ is the pump frequency.

Moreover, the radiation spectrum is completely tuneable in the VUV-XUV region by means of frequency-mixing techniques applied on the pump laser [9]. High harmonics are linearly polarized sources [10] of high temporal [11] and spatial [12] coherence, emitting very short pulses (less than 100 fs), with a relatively high repetition rate (up to MHz [13]). The harmonic radiation is emitted in the axis of the laser propagation with a small divergence (1 to 10 mrad).

## TECHNICAL REALISATION OF THE SEEDING WITH HH

The first specification is to use a femtosecond intense laser allowing to generate harmonics with as much as possible energy per pulse to overpass the SASE shot noise. Then these harmonics must be, using a restricted number of optics, refocalized inside the undulator system, taking advantage of a magnetic chicane, in order to adapt the harmonic divergence as closed as possible to the electron beam one. Also, both beams have to be precisely transversally overlapped all along the entire undulator and synchronized with subfemtosecond precision. Finally, the HH radiation must have the same polarization and the same wavelength as the undulator emitted light.

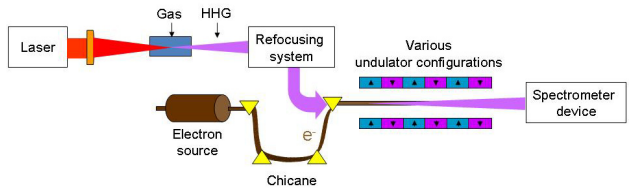


Figure 3: Scheme of a typical seeding experiment of a FEL with HH.

## PROOF OF PRINCIPLE EXPERIMENT: SEEDING WITH 160 NM RADIATION

The proof-of-principle experiment has been performed on the SCSS Test Accelerator in Japan in 2007 [14]. This facility is mainly based on a thermionic cathode electron gun (1 nC), a C-band LINAC (5712 MHz, 35 MV/m) and an in-vacuum undulator (15 mm of period, 2 sections of 4.5 m length). In June 2006, the first lasing has been observed at 49 nm and the full saturation has been reached in 2007.

It first showed that using 150 MeV electron beam the 5th harmonic of a Ti: Sa laser, at 160 nm, could be coherently amplified (figure 4), while the seeded energy per pulse was less than nanojoule level. The single shot seeded emission achieved four orders of magnitude higher intensity than the seed and a factor of 15 compared to the SASE, reaching in only one undulator section the microjoule level. Moreover, the corresponding spectral distribution presented a regular quasi perfect Gaussian shape.

Taking into account the pulse duration difference between the unseeded emission (0.3 ps-RMS) and the seeded one (46 fs-RMS), the strong spectral width reduction observed with seeding indicates that the temporal coherence is largely improved compared to SASE.

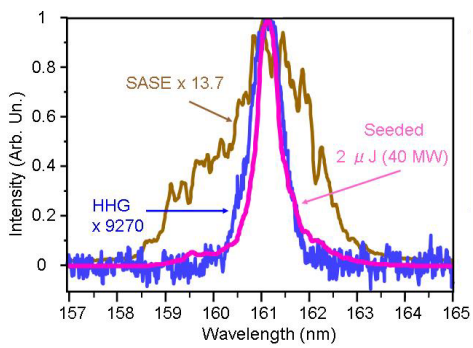


Figure 4: Single shot fundamental emission spectra in SASE, HHG and Seeding modes. One undulator section.



ISBN 978-3-95450-117-5

This amplification is accompanied by the generation of both odd and even coherent FEL non linear harmonics [15], from the 2nd to the 7th orders at 23 nm, while the energy of the electron beam is only here of 150 MeV. The NLH show similar spectral behaviors than the fundamental. Actually, operation of the FEL in the seeded configuration requires a fine synchronization between the laser pulse and the electron bunch arrival time in the undulator. To relax the synchronization requirement, the electron bunch was stretched. Also, in order to compare NLH in SASE and seeded modes, two undulator sections were used.

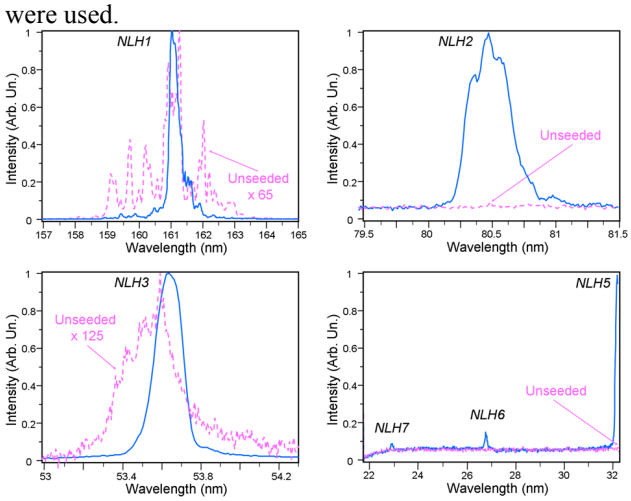


Figure 5 Single shot NLH spectra of the seeded (blue ---) and unseeded (pink - -) FEL. Electron beam in a stretched mode, $P_{seed}$=82 W, two undulator sections.

Figure 5 enables to compare the spectral content of the unseeded and seeded FEL. While in the unseeded case, no signal could be detected above the 3rd harmonic, in the seeded case, significant signals have been observed actually up to the 7th order. In that stretched case, the peak power is enhanced by a factor 65 on the fundamental and 125 on the 3rd harmonic. In addition, seeding clearly enables to remove the spiky structures of the spectrum and to obtain a nice Gaussian shape. The unseeded FEL delivers light pulses with a spectral width of 1.36% on fundamental and 1.27% on the 3rd harmonic. Due to seeding, the spectra are narrowed respectively by factor 4.5 and 3.8. Assuming that the unseeded FEL pulse duration is approximately equal to the electron bunch duration (0.8 ps-RMS), and that the seeded FEL pulse duration is approximately equal to the HHG pulse duration (46 fs-RMS), the reduction factor of the pulse duration due to seeding is about 17. Together with the spectral narrowing, the FEL gets significantly closer to the Fourier limit than the spontaneous emission (by a factor 70=3.8x17 in the case of the 3rd harmonic), corresponding to a strong improvement of the temporal coherence.

It was also report on the experimental distinction between the seed level influence on the spectral narrowing and shot noise overcoming [16]: a first threshold takes place for the seed level to overcome the shot noise and a second one corresponds to the improvement and control of the coherence properties. These two new seed levels are theoretically interpreted with respect to shot noise. They indicate how the FEL output can be controlled via the seed intensity and give precise scaling for new FEL sources at short wavelengths. The intensity distribution for particular seed energy values is displayed in figure 6. First, the FEL operates in the SASE regime with output energy $E_{FEL}$ below 1 nJ; the spiky spectrum corresponds to a weak temporal coherence. Then, with a seed energy of 1.4 pJ, a small amplification $E_{FEL}$=1.4nJ) occurs and the spectral distribution is smoothed out. Finally at 8.8 pJ, the radiation is amplified by one order of magnitude $E_{FEL}$ =12.2 nJ) and the spectrum exhibits a regular quasi Gaussian shape narrowed with respect to both the SASE and the seed ones. Seeding provides the FEL with a higher output power and an improved temporal coherence.

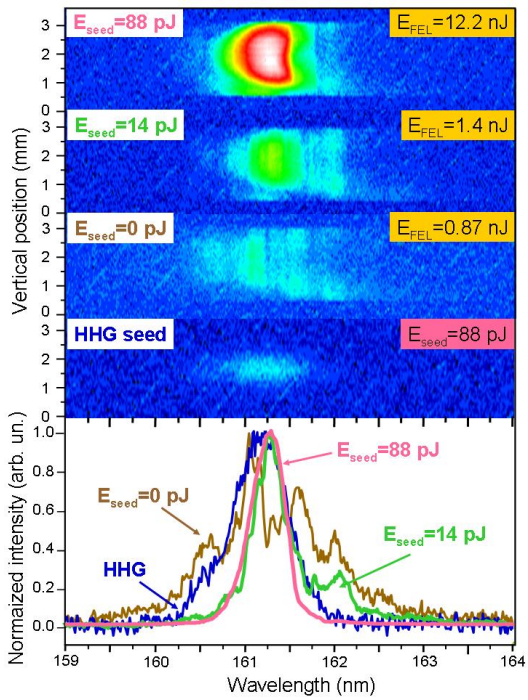


Figure 6: Top: Single shot emissions recorded on a spectrometer CCD camera: HHG seed ($E_{seed}$=8.8 pJ), unseeded FEL ($E_{seed}$=0 pJ) and seeded FEL with $E_{seed}$=1.4 and 8.8 pJ. $E_{FEL}$: FEL output energy per pulse. Bottom: normalised spectral intensities retrieved from the above images.

## RECENT ADDITIONAL SEEDING EXPERIMENTS

Last year, still on the SCSS Test accelerator, and after an upgrade of the laser system, the full energy of the electron beam, i.e. 250 MeV, has been used for the first time to amplify down to the 60 nm radiation [17], corresponding to the 13th harmonic of the laser. The seeded mode signal (figure 7) presents a Gaussian shape and has intensity higher than the unseeded signal by a factor of 5 approximately.

ISBN 978-3-95450-117-5

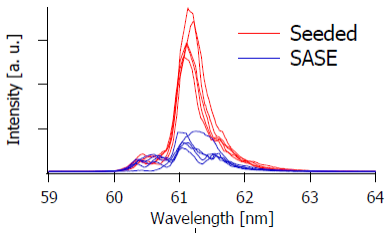


Figure 7: Spectra of the seeded and unseeded emission at 60 nm measured on the SCSS Test Accelerator.

Presently, other sites have implemented soon seeding schemes in their facilities as a main mode of functioning, such as the test-bed HH seeding facility SPARC (Italy), which has deliver photons in the VUV region down to 133 nm [18] (figure 8). Actually, this configuration is not a direct seeding but a HGHG system, where a second undulator section amplify the second harmonic of a first undulator section seeded here with the 3rd harmonic of the laser.

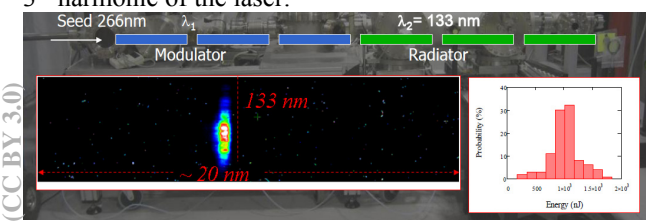


Figure 8: Seeding experiment at SPARC in HGHG configuration.

sFLASH (Germany) [19] is also now being designed and should operate in 2011 in the soft-X ray region from 30 nm to 13 nm.

## WHAT HAS TO BE IMPROVED ON HHG FOR SEEDING FEL?

### *Intensity, tuneability, wavefront*

As most of the applications are aiming in the wavelength range from soft to hard X-ray (20nm to 0.1 nm), valuable HH seed intensity is required in this spectral range, where unluckily the efficiency of the classical harmonic generation, from 800 nm Ti: Sa laser system, has a sharp decrease. Also, seeding with high harmonics should not have any constrain on the machine performances, such as the tuneability. This is why there is an urgent need of developing new HH sources, more intense at shorter wavelengths at high repetition rates and with larger tuneability. Harmonics generated in an orthogonally polarised two-colour laser field, consisting of mixing the fundamental frequency ($\omega$, actually the fundamental pulsation) and its second harmonic ($2\omega$), should fulfil all the above-mentioned seeding requirements.

First, contrary to classical harmonic generation both odd and even harmonics are generated (figure 9), corresponding to the odd harmonics naturally generated by $\omega$, but also by $2\omega$ ($2\times(2n+1)$), and to the harmonics coming from the mixing itself ($2\times(2n)$). Second, there is a "redshift" of the whole spectrum, i.e. a shifting to lower harmonic orders of the cut-off, the region where the number of photons start to decrease fast, which is unwished for a seeding. Third, the efficiency of generation can be highly increased.

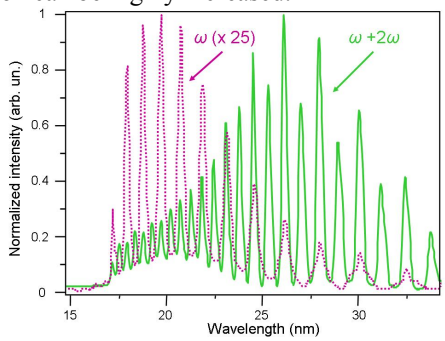


Figure 9: Normalised intensity HH spectra obtained with neon gas with either $\omega$ or $\omega$+$2\omega$ technique and with same optimisation parameters as for $\omega$ and 100 µm thick BBO.

The two-colour ($\omega$+$2\omega$) harmonic generation experiment has been performed at the Laboratoire d'Optique Appliquée (France) by means of a kHz Ti: Sa laser system at 800 nm ($\omega$) delivering maximum of 7 mJ energy in 35 fs FWHM (Full Width Half Maximum) pulses. Figure 10 presents a scheme of the set-up. In order to generate the 400 nm radiation ($2\omega$), a BBO (Beta Barium Borate, type 1) doubling crystal, is directly inserted in the IR beam path between a 1.5 m focusing lens and a gas cell (typically 4 to 7 mm long). In this geometry, the second harmonic component propagates along the same axis as the IR beam, and consequently the spatial overlap between the $\omega$ and $2\omega$ parts is automatically achieved in the active medium. Our frequency doubling geometric configuration is then completely straightforward and as a result, it can be easily implemented in HH seeding schemes.

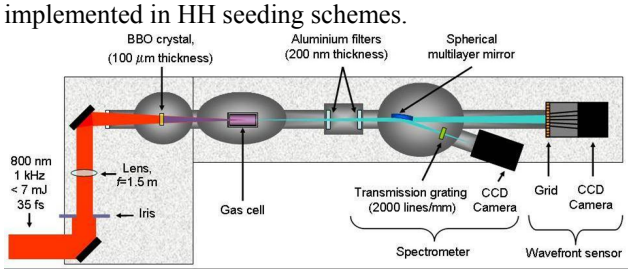


Figure 10: Layout of the kHz two-colour high harmonic generation experiment with a BBO crystal for measuring both the spectrum and the wavefront.

A detailed study of a high repetition rate harmonic generation source with two-colour mixing in many gases has been performed [20]. High factor of increase is here observed, when keeping the same optimisation parameters as for $\omega$. Spectra (figure 11) present a relatively flat distribution with an intensity ratio from odd to even harmonics close to one, and the intensification arises over the whole spectrum. Also this enhancement is clearly dependent on the considered gas (Fig. 4), typically He (×~100), Ne (×~25), Ar (×~0.5), Kr (×~0.5) and Xe (×~0.5). The high efficiency of this two-colour process at short wavelengths notably compensates



ISBN 978-3-95450-117-5

the low efficiency of the classical harmonic generation in this range. Consequently, it extends the spectral region accessible for applications and seeding to shorter wavelengths.

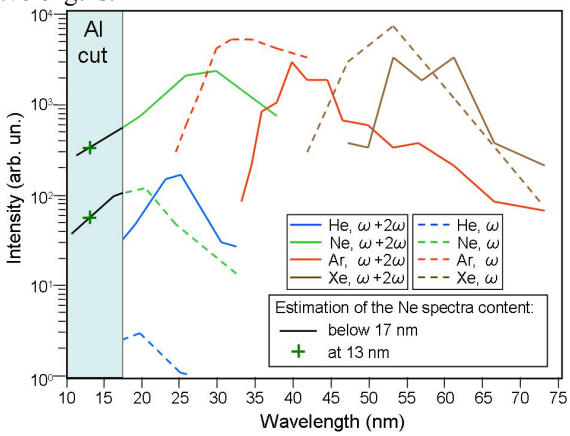


Figure 11: Schematic representation of the achieved experimental intensity for different gases. The curves presented match to the fitted envelope of the recorded spectra. The spectra have been obtained with either $\omega$ or $\omega$+2$\omega$ technique (100 µm thick BBO crystal) and with same optimisation parameters as for $\omega$.

Since the two-colour harmonic generation process is different from the standard one at the fundamental frequency, the optimal parameters for both cases have to be notably different. Figure 12 presents spectra and corresponded wave front [21] patterns of the HH source generated from argon gas target in various configurations to optimize both HH intensity and wave front.

First and foremost, just at $\omega$, the harmonic yield has been maximised by clipping the IR beam with an iris of 20 mm aperture. Compared to the fully open IR beam case (40 mm diameter at $1/e^2$), aberrations are decreased by a factor of 6, as the highest components of deformation located in the outer part of the driving laser beam are removed, to λ/6 rms ((2) with λ=37.5 nm, the first main component of the spectrum from red curve of (1)).

In contrast, the two-colour high harmonic generation for a full aperture beam delivers radiations with low aberration properties, λ/5 rms ((3) with λ=44.5 nm, the first major component of the spectrum from the blue curve of (1)), i.e. equivalent to three times the diffraction limit. Moreover high increase of the harmonic yield is observed, reaching tens of nJ per pulse for the 2x(2n+1) orders. Actually the parameters of harmonic yield optimisation for the mixing case are quite different from those employed before: 30 mbar to 16 mbar of pressure inside the gas cell and 8 mm to 4 mm of gas cell length.

Then, when clipping the IR beam with the same iris aperture as used for $\omega$ (20 mm), the generated harmonic beam is now totally free from aberration, with residual deformations at λ/17 rms ((4) with λ=44.5 nm), but the efficiency of generation partly decreased as the iris limits here the available blue energy. Such a very low aberration value has been explained with a spatial filtering of the driving laser wave front by the blue waist which is 1.4 times smaller compared to the IR one in our geometry. This has been proved by evaluating the HH waist values in both cases, accessible here by retro propagating the electric field from the wave front sensor, delivering the HH phase and intensity distribution.

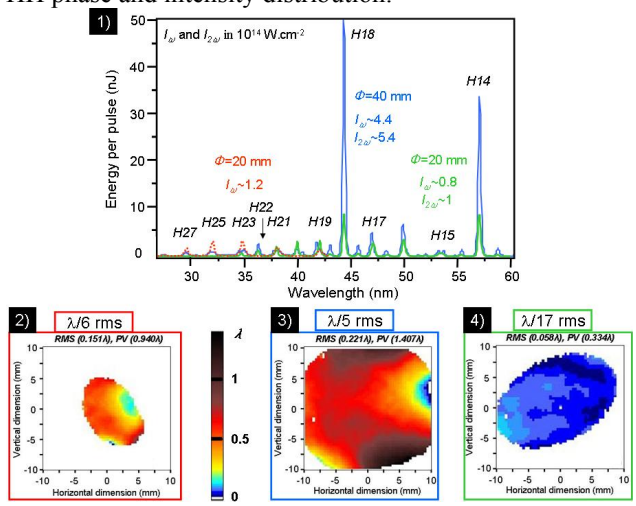


Figure 12: 1) Normalised HH spectra obtained in argon gas for different conditions of generation, either with $\omega$ or $\omega$+2$\omega$ and for different driving laser beam diameter apertures (Φ) and intensity at $\omega$ and 2$\omega$. Down: wave front distortion amplitudes recorded on the wave front sensor (λ($\omega$)=37.5 nm and λ($\omega$+2$\omega$)=44.5 nm). (2) $\omega$ technique, Φ=20 mm. (3) $\omega$+2$\omega$ technique, Φ=40 mm. (4) $\omega$+2$\omega$ technique, Φ=20 mm.

## *Variability of the Polarization*

Up to now, seeding has only been performed with linearly polarized HH light. Indeed, HH sources deliver linearly polarized light when a linearly polarized driving laser is focused into the atomic gas, as the high harmonic beam polarization follows the atomic dipole direction, which is directly related to the driving laser polarization. Several attempts have been made to obtain circularly polarized harmonics. It has been shown that using an elliptically polarized driving laser, the HH generation efficiency drops dramatically with increasing ellipticity of the driving laser [22]. More recently, elliptically polarized harmonics have been obtained in molecular gases [23], but the degree of circular polarization is low (<40%). In contrast to these previous reports, we chose a two-step procedure to obtain circularly polarized harmonics; first, linearly polarized harmonics are generated and second they are circularly polarized.

For wavelengths below 100 nm the lack of transparent materials prevents the fabrication of quarter-wave plates. The basic idea is then to use the phase-shift introduced between the s and p component of an electromagnetic wave by a reflection on a mirror. To produce circularly polarized light from linearly polarized light, first of all, a phase-shift of π/2 must be introduced. To obtain circularly polarized light, it is also necessary to

ISBN 978-3-95450-117-5

adjust the direction of polarization of the incoming light so that after reflection the s and p components have equal intensity. Since the phase-shift accumulates with each mirror, a smaller shift per mirror, hence, a smaller glancing angle can be used. This greatly improves the efficiency of the polarizer. As a consequence, a four mirror system (figure 13) optimized for a bunch of 8 harmonics from 18 nm to 26 nm [24] was used. The performance of the polarizer has been measured using a rotating analyzer consisting of a multilayer mirror set at an incidence angle of 45°. Close to 100% circularly polarized light can be obtained (figure 14) on this range. The measured transmission is about a few % (table 1).

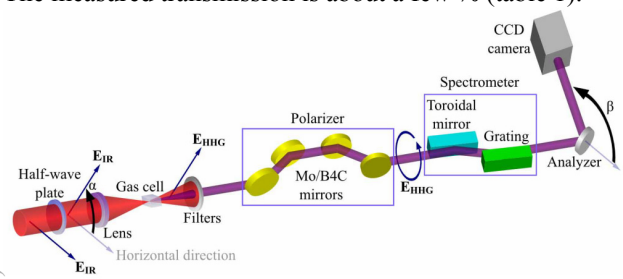


Figure 13: Setup layout showing the production of the harmonics in a neon filled gas cell, the polarizer, the spectrometer, the analyzer and the CCD camera.

Table 1: Efficiency of the polarizer in term of transmission ($T_C$) and circularity ($P_{Cmax}$) for 8 consecutive harmonics.

| Harmonic order | 31st | 33rd | 35th | 37th | 39th | 41st | 43rd | 45th |
|---|---|---|---|---|---|---|---|---|
| λ (nm) | 26.3 | 24.7 | 23.3 | 22 | 20.9 | 19.9 | 19 | 18.1 |
| $P_{Cmax}$ (%) | 100 | 100 | 97 | 91 | 85 | 76 | 66 | 61 |
| $T_C$ (%) | 2.6 | 2.7 | 3.7 | 3.6 | 4.4 | 4.3 | 4.0 | 3.7 |

## USER APPLICATIONS IN XUV: SASE-FEL VS HH

Generally speaking, both techniques are known to have their own limits and their particularities. In the one hand, the Attosecond science of HH is booming since the last ten years but the harmonics suffer from their low flux. On the other hand FEL have unique possibility to reach intense X-ray emission but in SASE configuration with low temporal coherence. Yet, looking at the XUV range the performances are relatively close to each other. and for experiments which do not need high number of photons, beam time access to harmonics is much easier.

Recently even single shot coherent diffraction imaging has been performed with HH (figure 14, [25]). In this experiment, 32 nm (20 fs, 1 μJ) radiation allows to "observe" an isolated nano-object, reconstructed with a resolution of 119 nm. For 5 accumulated shots the resolution increases to 62 nm.

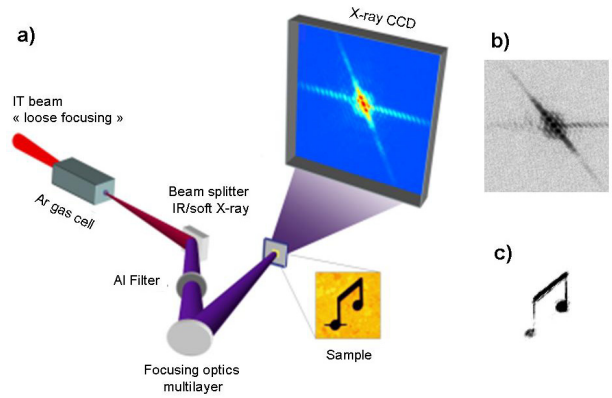


Figure 14: a) Layout of the coherent diffraction experiment of an isolated nano-object. b) Measured single shot diffraction pattern. c) Reconstructed nano-object.

The latest progress made on HH hence demonstrated that observing nano-structures of higher physical interest, such as magnetic domains, is now possible [26]. Indeed, coherent diffraction imaging experiment has been performed in which magnetic domains were probing with nanometer spatial resolution. Using a high throughput monochromator (figure 15), XUV pulses with a photon energy resonant to the magnetically dichroic Co $M_{2,3}$ absorption resonance were refocused onto a CoPd alloy film : a magnetic scattering pattern was recorded in a transmission geometry (figure 16). The scattering pattern induced by the magnetic domain structure consists of two well-defined bright spots revealing the presence of stripe domains of about 63 nm in width.

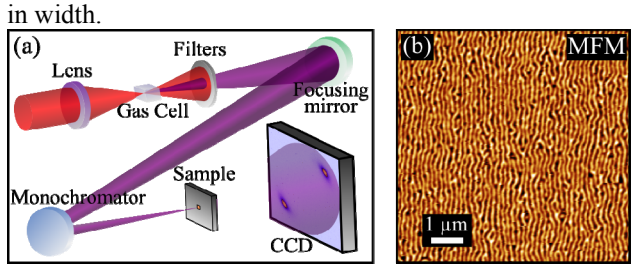


Figure 15: a) Layout of the coherent diffraction imaging experiments. b) Magnetic force microscopy (MFM) image of the sample showing the magnetic domain structure.

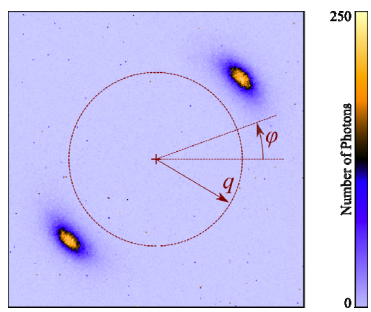


Figure 16: Resonant magnetic scattering pattern recorded on the CCD camera for an illumination time of 1200 s.



ISBN 978-3-95450-117-5

## ACKNOWLEGMENTS

The authors thank the support from the Laserlab Integrated Infrastructures Initiative RII-CT-2003-506350 and from the European Research Council Paris ERC project 226424. Financial support for this work was provided by the TUIXS European project (Table top Ultra Intense XUV Sources) FP6 NEST-Adventure n.012843.

## CONCLUSIONS AND PERSPECTIVES

In conclusion, even a low level HH seed enables a dramatic increase of the temporal coherence and a strong enhancement of the FEL nonlinear harmonics intensities extending the available spectral range and therefore leading to a significant increase of the number of possible FEL applications. The effect of seeding becomes significant when the seed level overcomes the electron beam shot noise. In the proof of principle experiment (150 MeV electron beam and radiation at 160 nm), the seed peak power was at least two orders of magnitude (82 W) higher than the shot noise (0.15 W). Scaling this result to a fundamental radiation at 10 nm ($80^{th}$ harmonics of a Ti:Sa laser) using 1 GeV electron beam energy, leads to a requirement on the seed peak power of less than 10 kW. Such a seed level has already been demonstrated even below 10 nm on a HH source [27]. This opens attractive perspectives for extending the seeded FEL spectral range to the X-ray domain.

In addition, with the progress of laser-based XUV sources, in terms of intensity at short wavelength, tunability, variability of the polarization, it gives bright outlooks for improved light sources. The jitter-free characteristic of the HH generation process which is of prime importance for high time resolution experiments, would be transferred to the FEL in case of seeding, giving bright future for this source. Besides, seeding also would benefit to user applications with the control of the spectral and temporal properties especially with a fundamental wavelength in the water-window region, the spectral region of major interest for biological studies, and with FEL nonlinear harmonics in the X-ray domain. Finally, such studies are also of interest for the highly probable next generation light source in which the electrons are accelerated by a plasma wakefield generated by an intense laser, naturally providing a synchronized seed, for a further control of the light source temporal coherence properties.

## REFERENCES

[1] R. Bonifacio et al. Opt. Commun. **50** 373 (1984).
[2] R. Bachelard et al. PRL **106** 234801 (2011).
[3] R. Ischebeck, NIMA **507** 417421 (2003).
[4] E. Saldin et al. Opt. Commun. **202** 169 (2002).
[5] L. H. Yu et al. Science **289** 932 (2000).
[6] K. Tiedtke et al. NJP **11** 023029 (2009).
[7] T. Shintake et al. Nature Photonics **2** 555 (2008).
[8] L. Giannessi et al. PRL **106** 144801 (2011).
[9] H. Eichmann et al. Phys. Rev. A **51** R3414 (1995).
[10] P. Salières et al. Adv. At. Mol. Opt. Phys. **41** 83 (1999).
[11] P. Salières et al. Science **292** 902 (2001).
[12] L. Le Déroff et al. Phys. Rev. A **61** 043802 (2000).
[13] J. Boullet et al. Optics letters, **34**, 1489 (2009).
[14] G. Lambert et al. Nature Physics **4** 296-300 (2008).
[15] T. Tanikawa et al. EPL **94** 34001 (2011).
[16] G. Lambert et al. EPL **88** 54002 (2009).
[17] T. Togashi et al. Optics Express **19** (1) 317-324 (2011).
[18] L. Giannessi et al. Proceedings FEL10, **1**, 4, JACOW (2011).
[19] J. Bodewaldt et al. Proceedings DIPAC09, **1**, 203, JACOW (2010).
[20] G. Lambert et al. NJP **11** 083033 (2009).
[21] G. Lambert et al. EPL **89** 24001 (2010).
[22] P. Dietrich et al. PRA **50** R3585 (1994).
[23] X. Zhou et al. PRL **102** 073902 (2009).
[24] B. Vodungbo et al. Optics express **19** (5) 4346 (2011).
[25] A. Ravasio et al. PRL **103** 028104 (2009).
[26] B. Vodungbo et al. EPL **94** 54003 (2011).
[27] B. Droomey et al PRL **99** 08001 (2007).

ISBN 978-3-95450-117-5